

The Potential of Computational Aeroelasticity in the Design Process of Helicopter Rotor Blades

Marcello Righi
Zurich University of Applied Sciences
Winterthur, CH
Email: marcello.righi@zhaw.ch

Abstract

This paper deals with development of a computational design tool, based on high-fidelity aerodynamic and structural models, able to provide a time-accurate dynamic response of a rotor in all possible flight conditions. The introduction of Computational Fluid Dynamics (CFD) in the prediction of the airloads acting on a rotor has shown significant progress in terms of accuracy with respect to more traditional analysis methods based on simplified / linearized aerodynamics. In order to provide accurate results, CFD analysis should adjust boundary conditions in accordance with the rigid and elastic motion of the blades. In most cases, this happens through a so-called weak-coupling technique, where CFD iteratively corrects the airloads based predicted with less sophisticated methods.

This approach has a number of limitations. *(i)* It is unsuitable to predict transient conditions such as the dynamic response to an initial disturbance, which might be used to investigate the dynamic stability in highly non-linear conditions. *(ii)* It has systematically failed to accurately predict phase angles. *(iii)* Strongly non-linear flight conditions can not be reliably simulated by means of Reynolds-Averaged turbulence models. *(iv)* It presents an extreme imbalance between aerodynamic and structural models as the blade is often represented as a bi-dimensional beam. *(v)* It relies in most cases on "rotorcraft" modules of mainstream CFD packages such as FUN3D or FLOWer. These software packages are used only by a small community and are therefore more expensive, less reliable and enjoy a smaller range of available features with respect to packages developed for larger communities of users.

The study documented in this paper starts from the observation that Computational Structural Dynamics (CSD) software has reached maturity and is widely adopted in industry, also in simulations coupled to CFD. Furthermore, the most recent versions of mainstream CFD packages include interfaces for CSD coupling and robust algorithms to dynamically deform the computational mesh. Two issues are addressed in this paper. The first one concerns the applicability of non-rotor-specific software tools to the investigation of rotor flow. The second issue deals with the capability of non rotor-specific software tools to help investigators removing the limitations mentioned above and providing the tools for a physically consistent and numerically accurate dynamic response. The results obtained after a preliminary study phase are discussed in the present paper.

1 Introduction

The flow around a rotor blade can be unsteady, three dimensional, transonic with shocks, possibly reversed. It can contain dynamic stalls and a vortical wake.

Its evolution depends not only on rigid motion of the blade but also on the elastic deformations. The fully coupled aeroelastic problem must account for the mutual dependence between structure and aerodynamics. Besides, the problem is strongly nonlinear: a small change in one of the design parameters might provide a significant change in the dynamic response.

Traditionally, rotorcraft industry has relied on the so-called comprehensive codes, which are based on a lifting-line representation of the blade aerodynamics and structurally on a bi-dimensional beam. It is

Level	Degrees of Freedom	Availability
2D aerodynamics, e.g. lifting-line, tables + prescribed wake	less than 100	rotorcraft comprehensive codes
Full potential + free wake	100'000 to one million	available on all CFD packages, CFD and CFD / CSD coupled simulations
Euler equations	100'000 to several million	available on all CFD packages, CFD and CFD / CSD coupled simulations
Laminar or Reynolds-Averaged Navier-Stokes equations	several million	available on all CFD packages, CFD and CFD / CSD coupled simulations
Large Eddy Simulation (time accurate Navier-Stokes equations, closed by sub-grid turbulence models)	several million	available on most CFD packages, no rotorcraft industrial applications known to the author

Table 1: Levels of sophistication in aerodynamic modeling

Level	Degrees of Freedom	Availability
Linear beam model, modal condensation	less than 100	CFD / CSD coupled simulations, rotorcraft comprehensive codes
Non-linear beam, multi-body	less than 100	CFD / CSD coupled simulations, rotorcraft comprehensive codes
High-fidelity Finite-Element-Model	up to several million	standard static and dynamic design tool, used in CFD / CSD coupled simulations (non-rotating frame)

Table 2: Levels of sophistication in structural modeling

recognized that the low fidelity of the models is the cause of the limitations in the capability to mimic the aerodynamic phenomena and their interaction with the rotor motion. This results in significant difference between predicted and measured airloads, especially on articulated rotors (i.e. where the motion is larger). In the last ten years a number of research projects have shown the superiority of a CFD-based approach, relying on inviscid aerodynamics ([9], [2]) or on the full Navier-Stokes set of equations closed with two-equation turbulence models ([5], [6], [8], [7]). These simulations could be placed in the second highest level of sophistication in aerodynamic modeling in table 1. The highest level has been reserved to Large Eddy Simulation, whose debut in aerospace has been announced several times but still has to happen. While the aerodynamic model uses millions of grid points, the structural model is four to five order of magnitude smaller. Structural models could only be placed in the lowest level of sophistication in table 2. This imbalance excludes from the analysis a number of non-linear aspects hidden in the (i) material behavior, (ii) geometry (for instance at blade tip but also at the root where large centrifugal tension loads is not everywhere parallel to carbon fibers roving), (iii) local instabilities, (iv) localized damage, (v) Free-play, (vi) Non-linear elements such as elastomeric dampers.

This paper is organized as follows. In order to explore the option of high-fidelity structural model, a commercial CFD / CSD software package, Ansys® has been tested, conducting a coupled simulation of a rotating tail rotor. The limitations of this approach are discussed and a more general CFD / CSD coupling framework is described, which leaves the users free to choose the preferred CFD and CSD tools. The handling of a rotating and deforming rotor blade - hence the suitability for rotor investigations - has subsequently been tested a well-known open-source CFD software package, OpenFOAM®¹. Finally, the role of turbulence models is investigated in a dynamic stall case and the "case" for Large Eddy Simulation

¹ OpenFOAM® is a registered trademark of OpenCFD

is briefly discussed.

2 CFD / CSD Coupled simulation of a rotating tail rotor

The first test addresses axial flight and has been conducted investigating the flow around a rotating tail rotor with the commercial code CFX®. Structures were modeled with Ansys®FEM. The coupled simulation has used the steady-state coupling included in the Ansys®package. The simulation has exploited the "turbomachinery" module of Ansys®, which has also been successfully applied to propellers. A two-bladed composite (glass and carbon fibers, radius $R = 1,20\text{ m}$, angular velocity $\Omega = 1'620\text{ rpm}$) tail rotor blade has been taken as test geometry.

The FE model includes about 140'000 nodes, 80'000 elements (SOLID187 and SHELL181) and can be considered as high-fidelity industry-standard (figure 1).

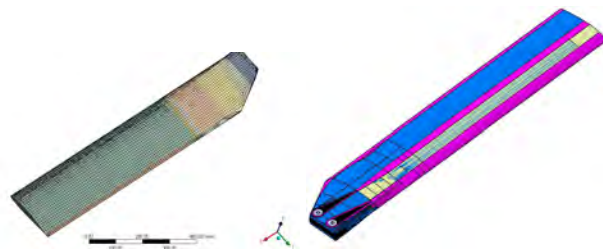


Figure 1: FEM model, skin (left) and view of the structural elements visible under the skin (right); colour scheme: pink, parts in glass fibers - blue, foam - light brown: parts in carbon fibers

Airloads have been calculated in a few axial flight cases. Figures 2 provide a few details of the aerodynamic mesh and a few qualitative views of the flow.

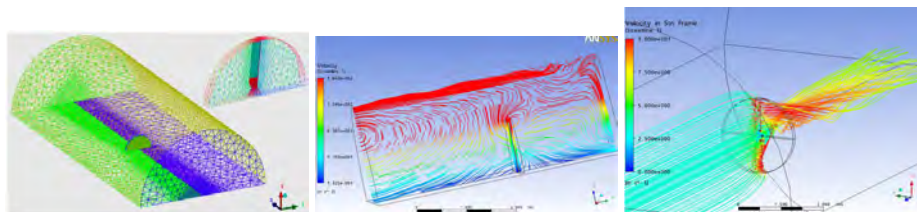


Figure 2: Views of the aerodynamic mesh and of the calculated flowlines

Figures 3 provides some views of the outcome in terms of stresses in the structural components.

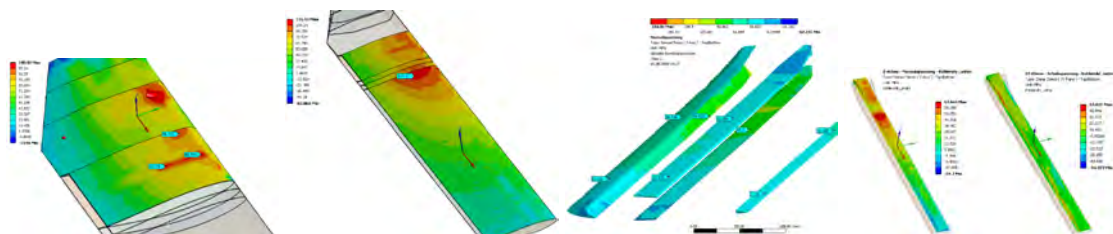


Figure 3: A few examples of the information provided, normal stress in the skin, normal and shear stresses in the glass fibers roving and in the carbon fibers longerons

This first test has demonstrated the feasibility of the application on a rotor. The out-of-the-box coupled system can be appreciated for its ease of use also with complex models. It could prove effective and efficient in the optimization of a few structural parts, such as glass fibers roving, for which loads experienced in axial flow are significant enough.

The test has also highlighted a few limitations. The most important is the difficulty of the system in handling large rigid flapping and, more in general, the high sensitivity to mesh quality. This makes it not the best option for design in general or optimization.

3 Time-accurate coupling between distinct CFD and CSD tools

In most rotor simulations periodicity is assumed and coupling is "weak", being information exchanged only once per revolution. Weak coupling is computationally more efficient than tight coupling and offers a greater flexibility in the choice of the CFD and structural tools.

However, this approach cannot handle transient conditions and is therefore unsuitable to compute dynamic responses for which a time-accurate coupling is necessary ([3]).

The fully coupled aeroelastic system is normally expressed in the form:

$$M\ddot{q} + B\dot{q} + Kq = f(u) \quad (1)$$

where q is the vector of the degrees of freedom, u are the flow fields, M , B and K are the mass, damping and stiffness matrices respectively. f is the vector of the aerodynamic forces. M , B and K are either the matrices generated from the FE discretization, if q are nodal coordinates or computed by means of the Lagrange's equations, in case of generalized degrees of freedom.

More in general we can define a CSD operator F_{CSD} :

$$q(t) = F_{CSD}(q(t_0), \dot{q}(t_0), \ddot{q}(t_0), f(t_0), \Delta t) \quad (2)$$

where t_0 is the time at the beginning of the simulation. A CFD operator, relating the flow fields u with q , would assume the form:

$$u(t) = F_{CFD}(q(t_0), \dot{q}(t_0), u(t_0), \Delta t) \quad (3)$$

Time-accurate coupling can be expressed for the generic time step Δt :

$$q(t_0 + \Delta t) = F_{CSD}(q(t_0), \dot{q}(t_0), \ddot{q}(t_0), f(t_0), \Delta t) \quad (4)$$

$$u(t_0 + \Delta t) = F_{CFD}(q(t_0), \dot{q}(t_0), u(t_0), \Delta t) \quad (5)$$

In practice the time step requirements for CFD are much more stringent than those for CSD. The second equation represents therefore more than one time step.

The vector f includes the operator which computes aerodynamic forces from pressure distribution. This operator depends on the choice of the structural degrees of freedom q and in practice is represented by an ad hoc interface software code. The present study does not yet include the development of the interface. the rest of the paper focuses instead on the choice of a suitable CFD tool.

Requirements for a physically accurate dynamic response of a rotating blade could be summarized:

- CFD can handle the motion of a blade in forward flight
- Mesh deformation algorithms are robust enough to cope with large flapping and lagging angles
- CFD tool can easily provide pressure distribution over blades
- CFD tool provides a number of compressible turbulence models which can be easily calibrated



Figure 4: Computational mesh at various times in one of the dynamic stall cases

As a first step towards dynamic response of a rotor in forward flight, the present study has assessed the open-source OpenFOAM® ([1]) as a potential CFD tool. Object of the assessment is the capability to handle a rotating blade solving the time-accurate compressible Navier-Stokes equations. The choice of OpenFOAM® is justified by the very effective and easy to use "dynamic mesh" functions, by the ease to code an ad-hoc interface and by the ample choice of validated turbulence models, which include Large Eddy Simulation.

4 Handling of dynamic mesh in OpenFOAM®

In general, blade motion includes the following components:

- Rigid rotation around the rotor mast at constant rotational speed ω
- Rigid flapping around the flap hinge with a prescribed amplitude $\beta = \beta_0 + \beta_{1c} \cos \omega t + \beta_{1s} \sin \omega t + \beta_{2c} \cos 2\omega t + \beta_{2s} \sin 2\omega t + \dots$
- Rigid lagging around lead/lag hinge with a prescribed amplitude $\zeta = \zeta_0 + \zeta_{1c} \cos \omega t + \zeta_{1s} \sin \omega t + \zeta_{2c} \cos 2\omega t + \zeta_{2s} \sin 2\omega t + \dots$
- Rigid pitch $\theta = \theta_0 + \theta_{1c} \cos \omega t + \theta_{1s} \sin \omega t$
- Elastic deformation of the blade: $\mathbf{e} = \sum A_{mn} \mathbf{f}_m e^{nj\omega t}$, where \mathbf{f}_i is a set of shape functions and A_{mn} a matrix of coefficients harmonic / shape function.

The following mesh solvers have been tested:

- velocityLaplacian
- displacementLaplacian
- displacementSBRStress

The "displacement" solvers have consistently provided the best compromise between mesh quality and computational cost. Mesh quality has been continuously monitored through the computation. A number of simulations have been conducted with different structured grid with various resolution and size. In all cases, a rapid calibration of grid and grid deformation parameters could provide an acceptable mesh quality throughout the simulation. As an example, figure 4 shows a 2D view of the computational mesh around the blade at various times of a dynamic stall simulation. Mesh skewness has kept constant at around 0.55 for one whole revolution.

Combination of rotation and deformation works well up to a specific azimuthal rotation, approximately 10 degrees for the velocity-based solvers and twice as much for the displacement-based ones.

Having generated the grid analytically, we have then "re-meshed" the computational domain every 10 or 20 degrees (and interpolated onto the new grid the flowfields computed so far).

Note that the most efficient way to manage the blade motion is to superimpose rigid rotation to elastic deformation and rotation around the blade hinges. This is possible with the use of libraries external (Suggar++) to OpenFOAM® but has not been tested here.

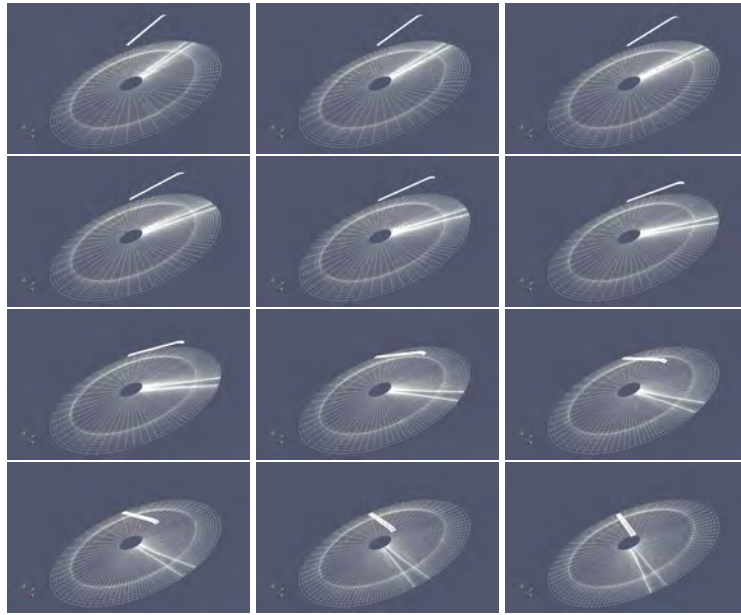


Figure 5: Rotation of the computational grid for around 100° used in a forward flight case, advance ratio $\mu \simeq 0.40$. The preservation of mesh quality has required a few re-meshing. Visualization obtained with ParaView 3.8.

Figures 5 and 6 show the computational mesh and vorticity at various times in a forward flight simulation at advance ratio $\mu \simeq 0.40$.

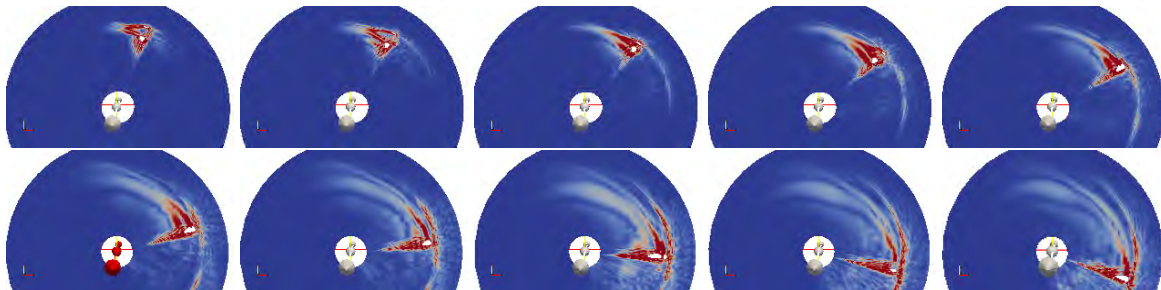


Figure 6: Vorticity on tip plane, horizontal flight, advance ratio $\mu \simeq 0.40$. Visualization obtained with ParaView 3.8.

5 Testing of some of OpenFOAM®'s features and early validation of the results

Validation is for the time being limited to the capability of CFD to correctly reproduce aerodynamic damping during a dynamic stall.

Two test cases have been considered: a mild and a strong dynamic stall. Both are taken from [10]. In the mild case a 0012 airfoil undergoes forced pitching oscillations according to:

$$\theta = 7.1^\circ + 8.4^\circ \sin \omega t \quad (6)$$

In the strong dynamic stall case, the forced oscillations are:

$$\theta = 10.3^\circ + 8.1^\circ \sin \omega t \quad (7)$$

In both cases, reduced frequency $k = 0.075$, Mach number $M = 0.40$.

In the first case a limited flow separation starts from the leading edge at a higher angle than that corresponding to static stall. As the airfoil reduces its angle of attack the flow gradually reattaches. Simulations have been carried out with two different turbulence models, $k - \omega$ and Spalart-Allmaras, obtaining comparable results, shown in figures 7, 8 and 9. In both cases, standard wall functions have been used. First gridpoint is located at around $y^+ \simeq 20 - 100$.

In the first, mild case, the agreement is only apparently good: the C_m hysteresis cycle is completed in clockwise sense (which corresponds to energy flow from the flow to the airfoil and has a destabilizing effect potentially leading to stall flutter) in reality, whereas the numerical simulation exhibits a counter-clockwise rotation sense. This is due to the fact that the CFD simulation predicts a too quick re-attachment of the flow.

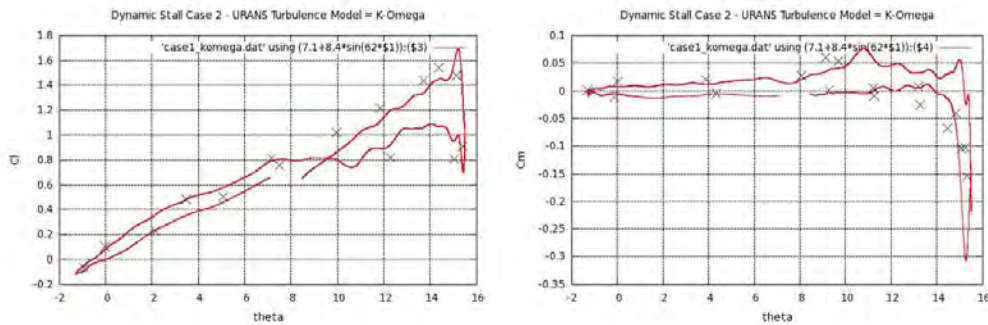


Figure 7: Mild dynamic stall. Turbulence model $k - \omega$. Normal force and moment coefficients as a function of pitch angle. 'x': experiment.

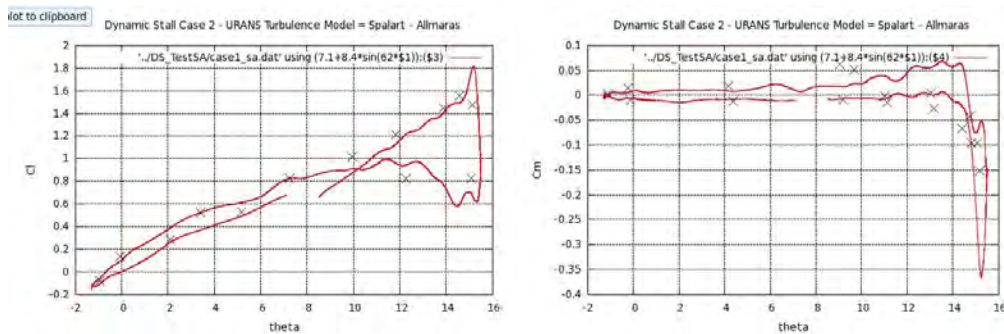


Figure 8: Mild dynamic stall. Turbulence model Spalart-Allmaras. Normal force and moment coefficients as a function of pitch angle. 'x': experiment

In the second, strong case, the agreement is not good because the numerical simulation fails to reproduce the correct re-attachment of the flow.

In both cases the differences between simulation and reality are due to the fact that the physics of the flow involves phenomena such as laminar to turbulence transition, laminar or turbulent separation and reattachment which cannot be represented by a single set of coefficients in the wall functions and in the turbulence model.

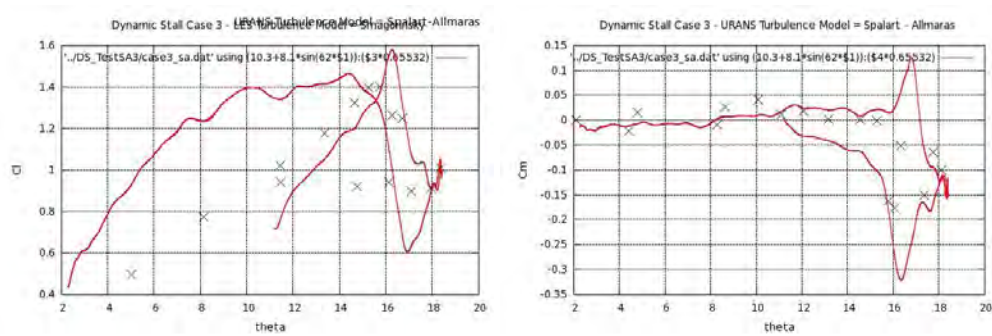


Figure 9: Strong dynamic stall. Turbulence model Spalart-Allmaras. Normal force and moment coefficients as a function of pitch angle. 'x': experiment.

The dynamic simulation could be set up and run on OpenFOAM® with no particular difficulties. A calibration of the turbulence models' coefficients could also be easily performed.

A successive validation exercise should include the assessment of the relation between wake capturing accuracy and adaptive mesh refinement.

6 A case for Large Eddy Simulation

A single turbulence model used in Unsteady Reynolds Averaged Navier-Stokes cannot be adequate for the whole flow domain because the mechanisms of turbulence production and dissipation are very different in flow regions and rotor working states such as in the attached or separated boundary layer on the blade, in the rotor wake, during blade-vortex interaction would require adjustable model coefficients

The same applies for Large Eddy Simulation sub-grid models but if large energy-carrying vortices are explicitly resolved the problem becomes less critical.

OpenFOAM® allows the user to perform Large Eddy Simulations of compressible flows with moving boundaries. Qualitative results are shown for a number of test cases.

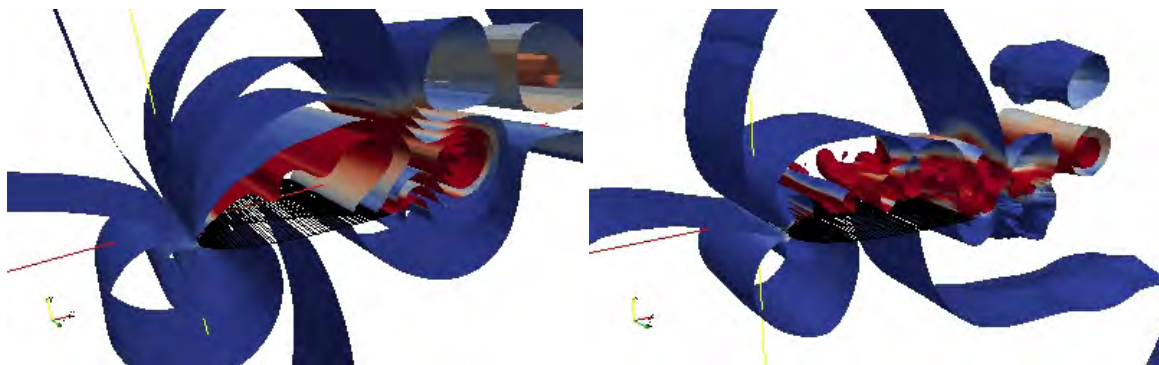


Figure 10: Strong dynamic stall test case run with URANS (Spalart-Allmaras) on the left hand side and with LES (Smagorinsky) on the right hand side. Visualization obtained with ParaView 3.8.

In figure 10 two screenshots of the strong dynamic stall case mentioned in the previous section are shown. One refers to the Unsteady Reynolds Averaged Navier-Stokes simulation mentioned. The second one has been obtained with Large Eddy Simulation. The two screenshots have been taken at the same simulation time. The comparison shows the large vortices being explicitly resolved by Large Eddy Simulation. The

simulation shows that the resolved vortexes have a life duration comparable with the blade passing period, introducing therefore frequencies comparable with the ones typical of blade dynamics (ranging broadly from 0 to a few times the blade passing frequency).

A final remark addresses the additional costs of Large Eddy Simulation with respect to Unsteady Reynolds Averaged Navier-Stokes. Additional spatial and temporal resolution is definitely necessary. However, this requirement might partially overlapping with the other stringent one to capture the rotor wake.

In figure 11 two simulations are compared. The initial conditions try to reproduce the separated flow that can develop in the "turbulent wake" working state of a rotor ([4]). The first one uses Unsteady Reynolds Averaged Navier-Stokes equations, whereas the second one is a Large Eddy Simulation. One can clearly see that in the second one, the simulation captures at least two sub-vortexes in the separated area.

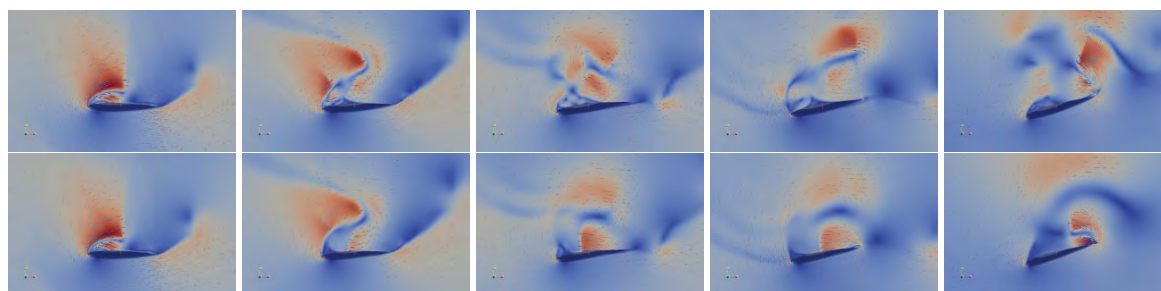


Figure 11: Vortex shedding from one blade in simulated "turbulent wake" working state, LES (above) and URANS (below) turbulence modeling techniques have been used starting the computation from the same initial conditions. Visualization obtained with ParaView 3.8.

7 Conclusions

This study has shown that the flow around a rotor in axial or forward flight can be numerically simulated with modern non rotor-specific CFD software packages, as they can effectively handle the rigid and elastic motion of the blade boundaries of the computational domain. Dynamic response of the rotor would require a time-accurate coupling with a high fidelity CSD model; this would require a relatively simple interface software code but not fully investigated in the present study.

Testing of an all-in-one solution, included in a commercial software package, has identified severe limitations in the ability to account for large rigid motion, typical of articulated rotors. The most interesting combination seems to be the coupling - through the ad hoc interface mentioned above - of the most appropriate CFD code with the most appropriate CSD code.

Unlike dynamic response which depends on the variation of aerodynamic forces in transient conditions, accuracy of airloads prediction - the most popular application of the coupled system - relies either on the resolution of the wake or on a free wake model. The necessary resolution and the related computational effort depends on the flight condition and might become extremely high if phenomena such as Blade-Vortex-Interaction (BVI) must be captured. Success depends therefore on features such as mesh refinement and overset grid - which are available in many CFD packages, including the two ones tested in this study.

Finally it is shown how modern CFD packages, the open source software OpenFOAM® in particular, are versatile enough to efficiently and effectively study "portions" of rotor flow and fine-tune the simulation parameters such as mesh resolution, mesh motion and turbulence models. It has been shown that ordinary turbulence models - calibrated for one particular type of turbulence - are unable to model the phenomena occurring during a dynamic stall in a dynamically accurate way.

Large Eddy Simulation (LES) could be easily applied to the study of dynamic stall and separated flow. Despite the fact that (uncalibrated) LES could not provide more accurate mean forces, it is shown that it

can provide much more information concerning the dynamics of the energy-carrying vortexes.

References

- [1] www.open CFD.co.uk.
- [2] ARM Altmikus, S. Wagner, P. Beaumier, and G. Servera. A comparison- Weak versus strong modular coupling for trimmed aeroelastic rotor simulations. In *AHS International, 58 th Annual Forum Proceedings-*, volume 1, pages 697–710, 2002.
- [3] G.P. Guruswarny. Computational-Fluid-Dynamics- and Computational-Structural-Dynamics-Based Time-Accurate Aeroelasticity of Helicopter Rotor Blades. *Journal of Aircraft*, 47:858 –863, 2010.
- [4] J.G. Leishman. *Principles of helicopter aerodynamics*. Cambridge Univ Pr, 2006.
- [5] K. Pahlke and B. Van Der Wall. Calculation of multibladed rotors in high-speed forward flight with weak fluid-structure-coupling. In *27th European Rotorcraft Forum, Moscow, Russia, 2001*.
- [6] K. Pahlke and B.G. Van Der Wall. Chimera simulations of multibladed rotors in high-speed forward flight with weak fluid-structure-coupling. *Aerospace Science and Technology*, 9(5):379–389, 2005.
- [7] H. Pomin, S. Wagner, and G. Stuttgart. Aeroelastic analysis of helicopter rotor blades on deformable chimera grids. & *Proceedings 40th AIAA Aerospace Sciences Meeting, Reno, 2002*.
- [8] M. Potsdam, H. Yeo, and W. Johnson. Rotor airloads prediction using loose aerodynamic/structural coupling. *Journal of Aircraft*, 43(3):732–742, 2006.
- [9] G. Servera, P. Beaumier, and M. Costes. A weak coupling method between the dynamics code HOST and the 3D unsteady Euler code WAVES. *Aerospace Science and Technology*, 5(6):397–408, 2001.
- [10] ME Wood. Results of oscillatory pitch and ramp tests on the NACA 0012 blade section. 1979.